Theoretical calculation

Methods. All density functional theory (DFT) calculations were performed using the Vienna Ab Initio simulation package (VASP).[1, 2] The electron-ion interaction was described with the projector augmented wave (PAW) method.[3, 4] The electron exchange and correlation energies were treated within the generalized gradient approximation in the Perdew-Burke-Ernzerhof formalism (GGA-PBE).[5] The plane wave basis was set up to 450 eV, and the Monkhorst-Pack k-point sampling was used. The k-point meshes used were determined by the size of the model, and provided in the following section. The convergence criteria for structure optimization and energy calculation were set to accurate quality with the tolerance for SCF and energy of 1.0 × 10^{-4} eV/atom.

The binding energy of the epoxy and hydroxyl functional groups on graphene was calculated with respect to the sum of energies of clean graphene and isolated O and OH in vacuum $E_{b1} = E_{GO} - E_X - E_G$, where E_{GO} and E_G are the total energy of graphene oxide and graphene, E_X is the energy of isolated O and OH. The binding energy of ferrous acetate ($Fe(CH_3COO)_2$), ferric hydrogen oxalate ($Fe(HC_2O_4)_3$) and ferric nitrate ($Fe(NO_3)_3$) was calculated according to $E_{b2} = E_{Fe-nY} - E_{Fe} - nE_Y$, where E_{Fe-nY} is the total energy of the compound of $Fe(CH_3COO)_2$, $Fe(HC_2O_4)_3$ and $Fe(NO_3)_3$. E_{Fe} is the energy of iron ions and E_Y is the energy of CH_3COO^-, $HC_2O_4^-$ and NO_3^-, with n the number of acetate, hydrogen oxalate, and nitrate anions. The adsorption energy of $Fe(NO_3)_3$, $Fe(HC_2O_4)_3$ and $Fe(CH_3COO)_2$ on graphene oxide was calculated according to $E_{ads} = E_{Fe-nY/GO} - E_{GO} - E_{Fe-nY}$, where $E_{Fe-nY/GO}$ is the total energy of graphene oxide with adsorbates in its equilibrium geometry, E_{GO} is the total energy of the graphene oxide, and E_{Fe-nY} is the total energy of the free adsorbates in the gas phase.

Models: Graphene oxide (GO) has a graphene carbon network with a random distribution of functional groups, and it is difficult to determine the accurate type and position of functional groups. Lerf et al[6 7] find graphite oxide (and thus likely GO) mainly has two types of functional groups: O bound in the C–C bridge site, and the hydroxyl (-OH) group. Guided by the findings by Lerf et al, we put forward a structure model of GO consisted of graphene (a sp^2-bonded hexagonal lattice), and the epoxy or hydroxyl functional group. In top views of graphene oxide, the unit cell p(4×4) were used. The 5×5×1 k-point sampling was set for the geometry optimization. A vacuum space (15 Å) was taken to prevent interlayer interactions. The structure of graphene oxide with three the epoxy functional group is given in **Fig S1**, which is the model to adsorb ferrous acetate, ferric hydrogen oxalate and ferric nitrate. The structure in p(8 × 8) unit cells was calculated. The vacuum region between slabs was around 15 Å, and Monkhorst Pack meshes of 3×3×1 k-point sampling in the Brillouin zone was used. The unit cells of $Fe(CH_3COO)_2$, $Fe(HC_2O_4)_3$ and $Fe(NO_3)_3$, as shown in **Fig S2**, were calculated, which contain one Fe atom and three NO_3 function groups, three HC_2O_4 (C_2O_4 in water), two CH_3COO. Our calculated lattice constant is a = 15 Å, b = 15Å, c = 15 Å, and $\beta = 90°$ and during the calculations, Monkhorst Pack meshes of 1×1×1 k-point sampling in the Brillouin zone were used.

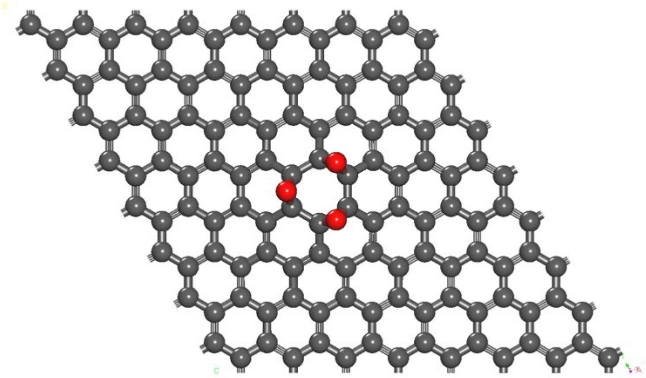

Fig S1 The structure of graphene oxide with three epoxide functional groups (carbon, oxygen atoms are given in gray, red).

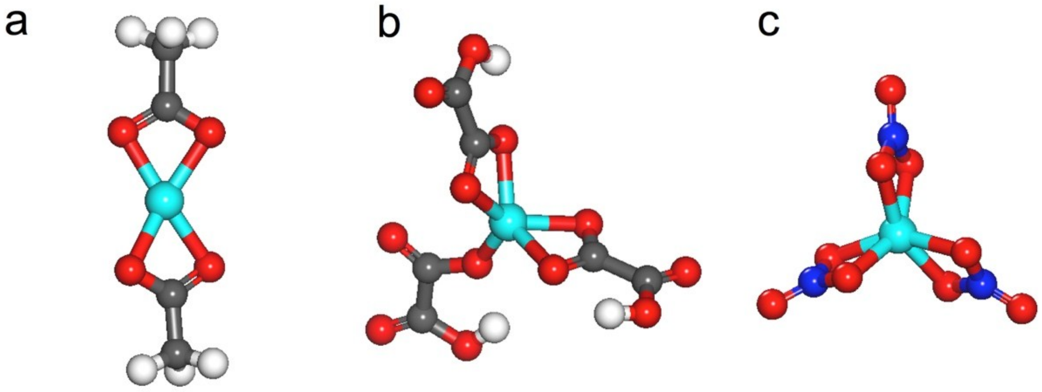

Fig S2 The structures of (a) ferrous acetate, (b) ferric oxalate, and (c) ferric nitrate (hydrogen, nitrogen, iron atoms are given in white, dark blue, and cyan).

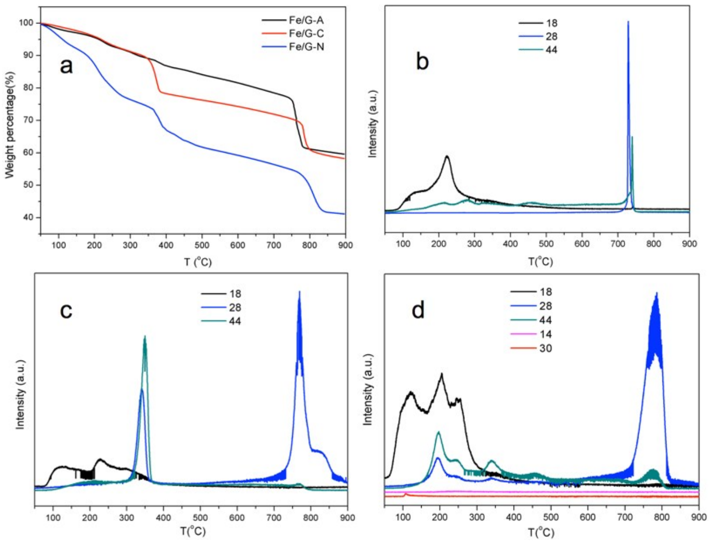

Fig S3 (a) TGA curves and corresponding mass spectra of released gas of the (b) Fe/G-A, (c) Fe/G-C, and (d) Fe/G-N catalysts.

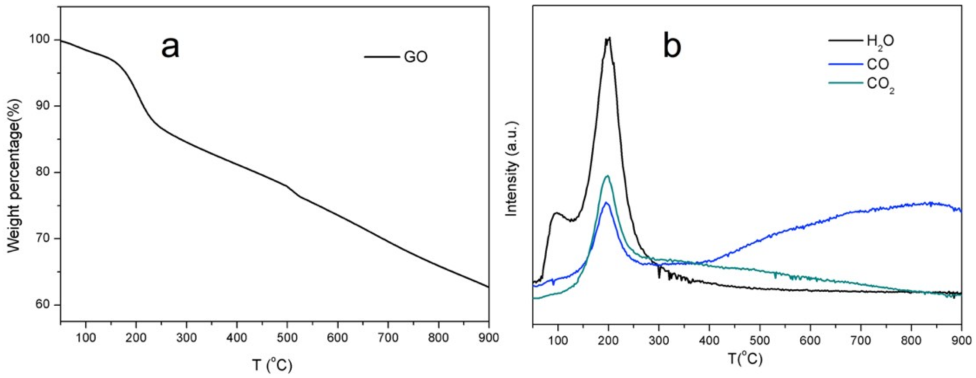

Fig S4 (a) TGA curves and (b) corresponding mass spectra of released gas of the GO after hydrothermal synthesis.

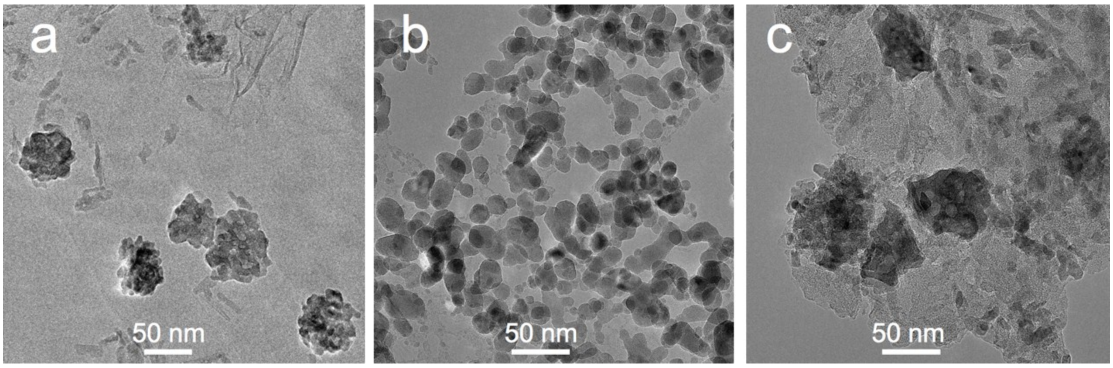

Fig S5 The TEM images of the (a) Fe/G-A, (b) Fe/G-C and (c) Fe/G-N catalysts.

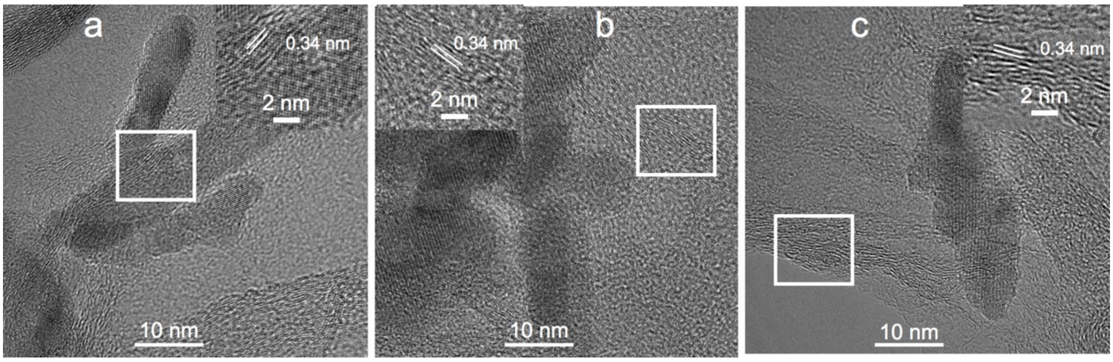

Fig S6 The HRTEM images of the (a) Fe/G-A, (b) Fe/G-C, and (c) Fe/G-N catalysts.

Fig S7 The optical photograph of sample after hydrothermal synthesis.

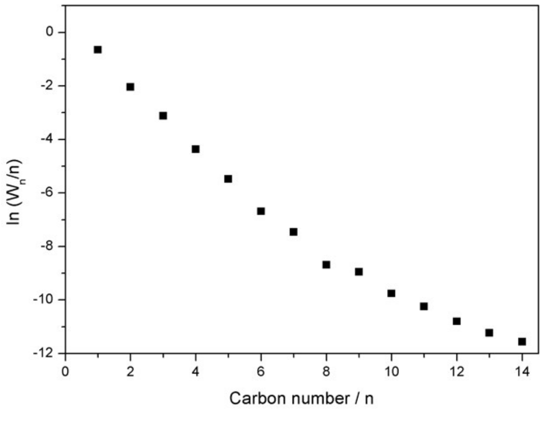

Fig S8 ASF plots of the prepared catalysts based on the product distribution after 24 h on stream.

Table S1 The surface elemental composition of catalysts determined by XPS analysis.

Catalysts	Fe (%)	C (%)	O (%)	N (%)

Fe/G-A	2.9	80.7	16.4	-
Fe/G-C	1.2	85.4	13.4	-
Fe/G-N	5.3	72.4	20.1	2.2

1. G. Kresse and J. Furthmüller, *Computational Materials Science*, 1996, **6**, 15-50.
2. G. Kresse and J. Furthmüller, *Physical Review B Condensed Matter*, 1996, **54**, 11169.
3. B. PE, *Physical Review B Condensed Matter*, 1994, **50**, 17953.
4. G. Kresse and D. Joubert, *Physical Review B Condensed Matter*, 1999, **59**, 1758-1775.
5. J. P. Perdew, K. Burke and M. Ernzerhof, *Physical Review Letters*, 1996, **77**, 3865-3868.
6. H. He, J. Klinowski, M. Forster and A. Lerf, *Chem. Phys. Lett*, 1998, **287**, 53-56.
7. A. Lerf, H. He, M. Forster and J. Klinowski, *J. Phys. Chem. B*, 1998, **102**, 4477-4482.